Finite-temperature properties of the two-dimensional Kondo lattice model

K. Haule

J. Stefan Institute, Jamova 39, 1000 Ljubljana, Slovenia

J. Bonča and P. Prelovšek

J. Stefan Institute, Jamova 39, 1000 Ljubljana, Slovenia
and FMF, University of Ljubljana, Ljubljana, Slovenia

Using the recently developed Lanczos technique we study finite-temperature properties of the 2D Kondo lattice model at various fillings of the conduction band. At half filling the quasiparticle gap governs physical properties of the chemical potential and the charge susceptibility at small temperatures. In the intermediate coupling regime quasiparticle gap scales approximately linearly with the Kondo coupling as $\Delta_{qp} \sim 0.3J$. Temperature dependence of the spin susceptibility seems to reveal two different temperature scales. A spin gap in the intermediate regime leads to a drop of the spin susceptibility at low temperatures, while a scaling of spin susceptibility is found for temperatures above $T_c \gtrsim 0.6J$. Charge susceptibility at finite doping reveals existence of heavy quasiparticles. A low energy scale is found at finite doping.

I. INTRODUCTION

The Kondo lattice model is one of the simplest two-band lattice models of correlated electrons. It is widely used to model heavy fermion materials where weakly interacting electrons in wide bands coexist with almost localized electrons in unfilled orbitals of actinide or rare-earth elements. In heavy fermion materials a remarkable variety of different phases can be found at low temperatures: paramagnetic metal with large quasiparticle mass, anti-ferromagnetic and ferromagnetic phases, unconventional superconductivity, etc. In most of these cases, strong electron correlations represent the key ingredient of the theory that explains the rich variety of physical phenomena.

In this work we investigate the Kondo lattice model, defined on a two dimensional square lattices. The model can be written as

$$H = -t \sum_{\langle \mathbf{ij} \rangle s} c_{\mathbf{i}s}^{\dagger} c_{\mathbf{j}s} + \text{H.c.} + J \sum_{\mathbf{i}} \mathbf{S_i s_i}, \qquad (1)$$

where $\mathbf{s}_i = \Sigma_{ss'} c_{\mathbf{i}s'}^{\dagger} \boldsymbol{\sigma}_{s's} c_{\mathbf{i}s}$ and summation $\langle \mathbf{ij} \rangle$ runs over nearest neighbors. There are two distinct types of degrees of freedom in this model: free electrons described by $c_{\mathbf{i}s}$ operators and localized spins described by $\mathbf{S_i}$. In the limit where $J=0$ two systems are decoupled which leads to a large degeneracy of states due to noninteracting spins. At finite Kondo coupling $J \neq 0$ the two systems interact. It is believed, that the interplay between the two degrees of freedom represents the most important physical mechanism of the heavy fermion materials. Associated with the two distinct systems are competing interactions that govern the low-temperature physics. Finite Kondo coupling leads to the formation of Kondo spin-singlets between the conducting electrons and the localized spins screening the magnetic moments of localized spins. Singlet formation competes with band propagation of electrons in the conduction band. Furthermore, localized spins interact via conduction electrons by the Ruderman-Kittel-Kasuya-Yoshida (RKKY) interaction that acts between localized spins. The Kondo screening and the RKKY interaction are in many cases competing interactions. Conditions, under which one or the other prevails depend mostly on the strength of the Kondo coupling, the electron filling and the dimensionality of the system.

A number of theoretical approaches has been applied to the investigation of the Kondo lattice model.[1] In the strong coupling regime perturbation theory can be applied.[2] Large-N_f expansion can be used in the case of large localized spin-degeneracy N_f.[3] The slave-boson approach,[4] Gutzwiller variational treatments,[5] and the recently developed strong coupling method[6] have been successful in predicting the heavy mass of the quasiparticles, the phase diagram, and the properties of the spectral functions.

Numerical calculations have been mostly limited to one dimensional systems where various well developed techniques are available and finite-size effects can be easily controlled. Calculations on small systems have demonstrated that at half-filling the one-dimensional Kondo lattice model is a spin liquid with a finite spin gap.[7] Density-matrix numerical-renormalization group (DMRG) calculations[8] provided an accurate determination of spin and charge gaps as a function of the Kondo coupling.[9,10] Recently, a powerful finite-temperature DMRG method[11,12] has been used to obtain results for thermodynamic[13–15] and dynamic properties[15,16] of the model at $T>0$.

While there are many reliable numerical results of the Kondo lattice model in 1D, much less is known about the model in two or three dimensions. Based on theoretical considerations conceptually different physical behavior is expected in higher dimensions. Spin-charge separation exists in 1D correlated models. Luttinger liquid parameters define power-law behavior of correlation functions in 1D while in higher dimensions exponential behavior of correlation functions is expected unless a long-range order exists. The lack of the long-range order in 1D is responsible for Kondo screening to overcome the RKKY interaction for any finite J.

In two dimensions, however, there is a critical value of $J_c/t \sim 1.4$ (Refs. 17–19) below which the RKKY interaction prevails and the system orders antiferromagnetically close to the half-filled conduction band.

The main purpose of this work is to explore thermodynamic properties of the 2D Kondo lattice model using the finite-temperature Lanczos method.[21] We focus our investigations to intermediate and high temperatures and try to identify energy and temperature scales that govern the spin and the charge response. Due to small system sizes we are not able to explore extremely low temperatures $T < T_{fs}$, since in this regime finite-size effects become dominant. For the same reason we limit our calculations to intermediate and strong coupling $J > t$ where physics is sufficiently local so that our results remain valid even in the thermodynamic limit.

II. ANALYTICAL APPROACHES

In this section we present results of two analytical approaches: (a) the high-T expansion up to the second nontrivial order in $1/T$ and (b) the atomic-limit, valid at large $J \gg t$. Despite their simplicity, these results nevertheless provide physical insight into two limiting cases and can be used as a guide to the interpretation of our numerical results.

A. High-temperature expansion

The grand-canonical sum can be written as

$$\Xi = \mathrm{Tr}\, e^{-\beta(H-\mu \hat{N})}, \tag{2}$$

where $\hat{N} = \Sigma_{\mathbf{i}} n_{\mathbf{i}}$ and $n_{\mathbf{i}} = \Sigma_s c_{\mathbf{i}s}^\dagger c_{\mathbf{i}s}$ is the fermion number operator, μ is the chemical potential and $\beta = 1/T$. $\exp(-\beta H)$ is expanded in powers of $1/T$ taking into account that at fixed particle density $\exp(\beta \mu \hat{N})$ is not a small number even at high-T. Equation (2) can be in the case $[H,\hat{N}]=0$ expressed in terms of cumulants as

$$\ln \Xi = 2N_s \ln(1+e^{\beta \mu}) + \sum_{n=1}^{\infty} \frac{(-\beta)^2}{n!} \langle H^n \rangle_c, \tag{3}$$

where $\langle \cdots \rangle_c$ symbolizes cumulants[20] and N_s is the number of lattice sites. Performing the cumulant expansion to β^2 we obtain

$$\ln \Xi \simeq -2N_s \ln(1-p) + \frac{\beta^2}{2} N_s p(1-p)\left[\frac{3J^2}{8} + 8t^2\right], \tag{4}$$

where $p = 1/[1+\exp(-\beta\mu)]$. Our calculations are performed at fixed particle density n, so the chemical potential $\mu(\beta,n)$ is calculated from the equation of the state

$$n = \frac{1}{N_s} \frac{d \ln \Xi}{d(\beta \mu)}. \tag{5}$$

After inverting and taking into account Eq. (4) leads to

$$\mu \simeq T\left[\log \frac{1-\delta}{1+\delta} - \frac{\delta}{2T^2}\left(\frac{3J^2}{8} + 8t^2\right)\right], \tag{6}$$

where we have introduced the doping $\delta = 1-n$. While the first term is model independent, the second one represents a nontrivial finite-temperature correction.

The charge response of the system can be measured with charge susceptibility $\chi_c = -d\delta/d\mu$ which can be expressed as

$$\chi_c \simeq \frac{1-\delta^2}{2T}\left[1 - \frac{1+\delta^2}{8T^2}\left(\frac{3J^2}{8} + 8t^2\right)\right]. \tag{7}$$

We evaluate the spin susceptibility via $\chi_s = \beta \langle S_{\mathrm{tot}}^z{}^2 \rangle$ and perform the high-temperature expansion

$$\chi_s \simeq \frac{3-\delta^2}{8T}\left[1 - \frac{1-\delta^2}{3-\delta^2}\frac{J}{2T}\right]. \tag{8}$$

Note, that unlike in the case of χ_c, there is a $1/T^2$ correction in χ_s.

B. Atomic limit

At large $J \gg t$, where the spin singlets that form between the electrons in the conduction band and localized spins are quite local, many physical properties of the model can be computed taking into account only a single lattice site. In this limit the grand canonical sum can be calculated as $Z = \Sigma_{j=1}^{8} e^{-\beta(E_j^{at}-\mu N)}$, and only 8 states are taken into account: the singlet state with the energy $E_{S=0}^{at} = -3J/4$, the degenerate triplet state $E_{S=1}^{at} = J/4$ both containing one conduction electron, and fourfold degenerate states $E_{S=1/2}^{at} = 0$ consisted of an empty and a doubly occupied conduction level each of them with two different spin configurations. Values of the spin, quasiparticle and charge gap are in this limit given by $\Delta_s = J$, $\Delta_{qp} = 3J/4$, and $\Delta_c = 1.5J$. For simplicity we present analytical results for spin and charge susceptibility only at zero doping ($\delta = 0$)

$$\chi_s = \beta \frac{1 + 2e^{-\beta J/4}}{4 + 3e^{-\beta J/4} + e^{3\beta J/4}}, \tag{9}$$

$$\chi_c = \beta \frac{4}{4 + 3e^{-\beta J/4} + e^{3\beta J/4}}, \tag{10}$$

where β is the inverse temperature and $\mu = 0$. At finite doping results cannot be written in an explicit form due to $\mu \neq 0$. However, in the low-T limit approximate results at $\delta \neq 0$ can be obtained

$$\chi_s \simeq \frac{\delta}{4T}, \tag{11}$$

$$\chi_c \simeq \frac{\delta(1-\delta)}{T}. \tag{12}$$

At $\delta \neq 0$ spin and charge susceptibilities diverge at low-T. χ_s diverges because interactions between moments on different atomic sites are negligible. χ_c diverges because of discrete energy levels at $J \gg t$.
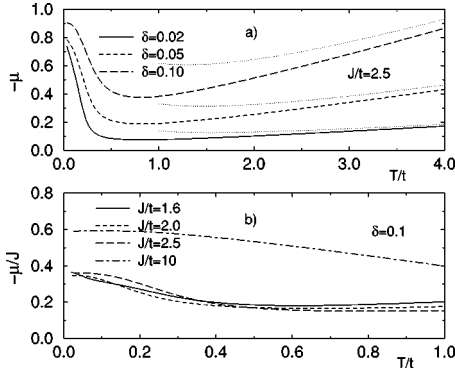
FIG. 1. Chemical potential μ as a function of temperature T; (a) at different dopings δ and fixed J, (b) at fixed doping δ and different couplings J/t.

III. RESULTS

Our numerical calculations are performed by recently developed finite-temperature Lanczos method.[21] We investigate square lattices of $N_s = 8$ and 10 sites. Most of the results presented are for the $N_s = 10$ case. Standard $T=0$ exact diagonalization results on small clusters are generally plagued by strong finite-size effects. Performing calculations at $T>0$ and within the grand-canonical ensemble gives us not only the thermodynamical properties of the system, but most importantly diminishes finite-size effects for $T>T_{fs}$.[21] The finite size T_{fs} depends primarily on the number of low lying excited states in the system. The T_{fs} can be quite small when the system possesses either (a) a large number of low-lying energy states or (b) if the physics is sufficiently local. A local physics is expected at large $J \gg t$ where the size of the Kondo singlet is of the order of lattice spacing. We present results for half-filled case $n=1$ and at finite doping $\delta \neq 0$. Due to particle-hole symmetry only $\delta > 0$ is considered. In this work we restrict calculations to thermodynamic quantities as are μ, χ_s, χ_c and the specific heat $c_v = -T \partial^2 F / \partial T^2$, where F is the free energy. Despite small system size we can compute thermodynamic quantities at any doping δ simply by choosing the appropriate chemical potential.[21]

A. Chemical potential μ

In Fig. 1(a) we show chemical potential μ as a function of T for small doping values and $J/t = 2.5$. Due to the particle-hole symmetry the relation $\mu(\delta=0)=0$ is valid at all T. At $T \gg t, J$ and $\delta \neq 0$, μ approaches the expression (faint dotted lines), calculated by the high-temperature expansion (6). Numerical results start deviating significantly from (6) below $T/t \sim 2$. At small T μ approaches a finite value even in the limit $\delta \to 0$. Infinitesimally small doping thus leads to an abrupt change of the chemical potential. Such behavior indicates formation of the quasiparticle gap Δ_{qp} also found in the 1D DMRG calculations.[14] To investigate the quasiparticle gap in more detail, we present in Fig. 1(b) μ/J at fixed doping for different choices of J on a system of $N_s = 10$ sites. We find that Δ_{qp} increases almost linearly with J in the intermediate coupling range, i.e., for $J/t = 1.6$, 2.0, and 2.5. Extrapolated values of Δ_{qp} in the $T \to 0$ limit are presented in Table I for systems of $N_s = 8$ and 10 sites. Results, obtained from the two systems agree reasonably well in the interme-

TABLE I. The quasiparticle gap Δ_{qp}/J and peak positions T_{qp}/J and T_s/J both presented in units of the Kondo coupling J. Quasiparticle gaps were obtained from the limit $\mu(\delta \to 0, T \to 0)$. Spin susceptibilities χ_s can be in the temperature interval $T/J < 0.6$ and for $J/t \leqslant 2.5$ well fitted to a simple form $\chi_s = C/T \exp(-T_s/T)$ where the effective moment C varies from 0.25 for small J/t to 0.5 at large J/t. Estimated errors where not otherwise specified are within 5%.

J/t ($N_s = 8$)	Δ_{qp}/J	T_{qp}/J	T_s/J
1.2	0.27	0.31	0.08 ± 0.04
1.6	0.28	0.30	0.13 ± 0.03
2.0	0.30	0.31	0.18 ± 0.03
2.5	0.32	0.31	0.31 ± 0.03
10.0	0.56	0.38	0.47 ± 0.04
J/t ($N_s = 10$)	Δ_{qp}/J	T_{qp}/J	T_s/J
1.2	0.40	0.49	0.09 ± 0.04
1.6	0.30	0.35	0.15 ± 0.03
2.0	0.29	0.32	0.23 ± 0.03
2.5	0.31	0.32	0.30 ± 0.03
10.0	0.56	0.38	0.47 ± 0.04

diate coupling range. In the strong coupling limit, e.g., $J/t = 10$, the extrapolated values agree well with the strong coupling result $\Delta_{qp} = \frac{3}{4}J - 2t + \frac{13}{6}t^2/J = 5.72$.[1]

B. Spin and charge susceptibilities

1. Zero doping

In Fig. 2(a) we present spin susceptibilities $J\chi_s(T/J)$ at zero doping, $\delta = 0$, for different values of J. At $T > t, J$ numerical results agree with the high-T expansion given by Eq. (8). In the intermediate temperature regime we find rather surprising result. All curves merge on a single curve for $T > T_c \sim 0.6J$. It could be argued that this is because the high-T result in Eq. (8) scales with J, i.e., the function $J\chi_s(J/T)$ is
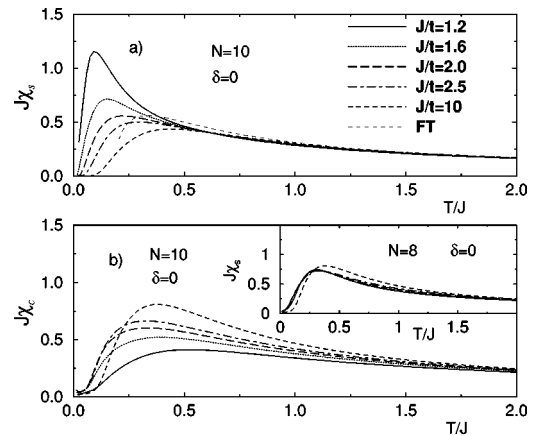

FIG. 2. Spin (a) and charge (b) susceptibilities $J\chi_s$, $J\chi_c$ vs T/J at zero doping. Faint dashed line in (a) represent high-temperature expansion result, Eq. (8). Legends, given in (a) apply also for (b) and the inset in (b). In the inset in (b) all six different curves for $J/t = 1.2-10$ are presented. All, except for $J/t = 10$ appear as a single line. Legend FT in (a) indicates analytical result, Eq. (8).

independent of J. However, the agreement with the Eq. (8) is only within 10% up to $T/J \sim 1$ [see Fig. 2(a)] while the overlap of susceptibilities calculated for a wide range of J/t is within a few percent. At low-T, χ_s reaches a maximum at $T = T_s$ and then approaches zero. In the strong coupling limit the spin gap Δ_s is larger than Δ_{qp}, however, at smaller J/t this is no longer true. In the region of small $J/t \sim 1.4$ Δ_s is expected to vanish due to formation of AFM order.[19] Low temperature behavior of χ_s in the intermediate coupling regime is thus governed by the spin gap. There are two possible approaches to estimate Δ_s using our method. At $T = 0$ Δ_s equals the energy difference between the lowest ($S = 0$) and the first excited ($S = 1$) state. At $T \neq 0$ the Δ_s can be estimated from the position of the peak in $\chi_s(T)$ given by the activation temperature T_s. We believe, that the second method, even though indirect, gives results that are closer to the thermodynamic limit.

Values of T_s are presented in Table I. As seen from Fig. 2(a) with increasing J, low-temperature peak in spin susceptibility moves toward higher values of T/J. T_s therefore does not scale linearly with J for small J as does Δ_{qp} (see Table I). This points towards a non-linear dependence of Δ_s vs. J/t that was found in 1D system[1] and also recent calculations in the 2D system.[19] A qualitatively good agreement is found also between T_s and the Δ_s obtained by the projection quantum Monte Carlo simulations.[19]

At small values of the Kondo coupling $J/t < 1.4$ gapless AFM long range order is expected to develop as a consequence of RKKY interaction.[18,19] Uniform spin susceptibility in this case saturates around the temperature which is given by the RKKY interaction between localized spins. Our results in this regime are less reliable at low-T due to pronounced finite-size effects.

The charge susceptibility χ_c shows in many respects different behavior than χ_s. The agreement of numerical results with the high-temperature expansion depends strongly on J. In Fig. 2(b) we show $J\chi_c(T/J)$ at $\delta = 0$ and a wide range of J. At large $J/t = 10$, where J is the dominant energy scale in the system, numerical results agree with the analytical result, given by Eq. (7), down to $T/J = 0.4$. At smaller J high-temperature limit is reached above $T/J > 2$.

χ_c is governed by a single energy scale, i.e., the quasiparticle gap Δ_{qp}. This is reflected in nearly perfect scaling of $J\chi_c(T/J)$ for the $N_s = 8$ system in the intermediate coupling region $1.2 \leqslant J/t \leqslant 2.5$ [see the inset of Fig. 2(b)]. Scaling is due to the fact that the quasiparticle gap scales nearly linearly with J, i.e., $\Delta_{qp} \simeq 0.3J$ in this regime. Δ_{qp} remains finite even at small $J \sim 1.2$ where the spin gap disappears. The scaling does not persist up to the strong coupling limit, $J/t = 10$ due to a crossover where Δ_s becomes larger than Δ_{qp}. The location of the peak at $T = T_{qp}$ seen in $\chi_c(T)$ matches the value of the quasiparticle gap $T_{qp} \sim \Delta_{qp}$ obtained from the doping dependence of the chemical potential (see Table I). Despite a smaller system size we believe, that near or at zero doping, $N_s = 8$ system shows less finite-size effects then the $N_s = 10$ when calculating quasiparticle properties of the system. The reason is that the $N_s = 8$ noninteracting fermion system has a sixfold degenerate level at zero energy which overlaps with the value of the chemical potential at zero doping. In contrast, the $N_s = 10$ noninteracting

system has a large gap at μ. The scaling is therefore less obvious for the $N_s = 10$ system size, however, locations of the peaks nevertheless approximately scale with J and peak positions T_{qp} approximately match Δ_{qp} obtained from μ for $J = 1.6$, 2.0, and 2.5.

2. Finite doping

Spin susceptibility χ_s, presented in Fig. 3(a), at small doping $\delta = 0.1$ show a similar high-temperature behavior as in the zero doping case. At $T \gg t, J$, χ_s follows Curie-like $1/T$ behavior, predicted by the high-T expansion, Eq. (8). As in the $\delta = 0$ case, χ_s curves calculated for different J/t show scaling above $T > T_c \sim 0.6J$. With decreasing temperature χ_s reaches a peak at $T = T_s$ where T_s is close to its $\delta = 0$ value. Even though Δ_s is expected to disappear at $\delta \neq 0$ and $T = 0$, at $T > 0$ remains of the spin gap can be observed. Similar results were observed in 1D calculations.[14] With further decreasing of T χ_s first decreases and then sharply increases at even lower temperature. In this region the susceptibility curve can be fitted to a simple form $\chi_s = C\delta/T$. This Curie-like form suggests that finite doping produces nearly free localized spins. In contrast to 1D results,[14] we find that for intermediate values $J/t = 1.6$, 2.0, and 2.5 the local moment is reduced and equals $C \sim 0.18$. In the strong coupling limit, $J/t = 10$, the local moment reaches its maximum value $C = 0.25$. In the extreme low-temperature limit χ_s should saturate either due to RKKY interaction between localized spins for small values of J/t or due to Kondo screening effects for larger J/t. This effect can be seen in the case of larger $\delta = 0.2$, where for intermediate $J/t = 1.6$, 2.0, and 2.5 χ_s shows less divergent behavior as in the $\delta = 0.1$ case.

The charge susceptibility χ_c at $\delta = 0.1$, presented in Fig. 3(b), follows the $1/T$ behavior at high-T, predicted by the expansion in Eq. (7). χ_c reaches a local maximum around $T = T_{qp}$. For small doping T_{qp} overlaps with its value at $\delta = 0$. At even smaller T we observe a sharp increase in χ_c. $\chi_c(T = 0)$ should be proportional to the quasiparticle mass. The sharp increase of χ_c therefore suggests that quasiparticles are very massive.

3. Comparison with the strong coupling results

At large values of J, physics of the Kondo model becomes local. We support our claim by results shown in Fig. 4 where we present comparison of χ_s and χ_c for $J/t = 10$ and analytical results obtained within the atomic limit. Spin and charge susceptibilities, Eqs. (9),(10), presented in Fig. (4) follow $1/T$ law at $T \gg J$. At lower temperatures we see a peak, marked by arrows. We introduce two temperature scales that mark the peak positions: $T_s = 0.453J$ and $T_{qp} = 0.386J$ for spin and charge susceptibility, respectively. Given values are obtained analytically from Eqs. (9),(10). At low-T both susceptibilities approach zero at $\delta = 0$ consistent with the existence of a gap in the excitation spectrum. Low-T behavior is in both cases given by $\chi_{c,s} \propto \beta \exp(-3\beta J/4)$ which leads us to a conclusion, that the quasiparticle (smallest) gap $\Delta_{qp}/J = 3/4$ governs the low-T behavior of both susceptibilities. This is possible since a quasiparticle excitation modifies the charge configuration and also changes the spin quantum number by $\pm 1/2$. Even though both susceptibilities share a common gap, they reach a maximum at slightly different
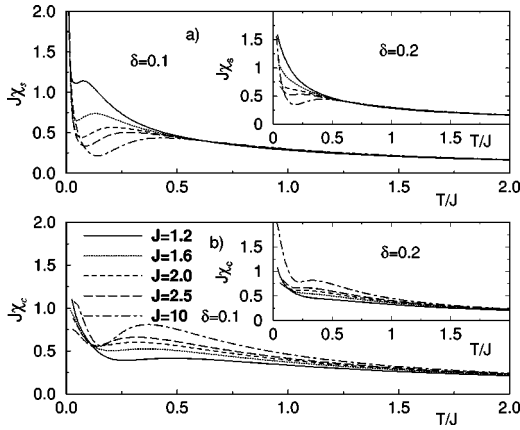
FIG. 3. Spin (a) and charge (b) susceptibilities $J\chi_s$, $J\chi_c$ vs T/J at $\delta = 0.1$ and 0.2. Legends given in (b) apply also for (a) and both insets.

temperatures T_s and T_{qp} which is due to different nature of the excitation spectra above the gap.

We see that numerical calculations at large $J/t = 10$, also presented in Fig. 4, agree reasonably well with analytical results at zero and finite doping. Agreement at finite doping is somewhat surprising since in the atomic limit only a single site of the Kondo lattice is taken into account. The divergence of spin and charge susceptibilities at low temperatures can be explained within the atomic limit, see Eqs. (11),(12). Divergence at low temperatures is in the strong coupling regime a consequence of nearly degenerate level system. At even lower T, results saturate towards finite values due to weak interatomic correlations that lift the degeneracy. In χ_c such a deviation from the predicted $1/T$ law can be seen in Fig. 4(b) while in χ_s such deviation is expected at even lower T.

C. Specific heat

Results for the specific heat c_v are shown in Fig. 5. At $J/t = 0$, c_v has a peak at finite T as for free conduction electrons. The contribution of localized noninteracting spins is
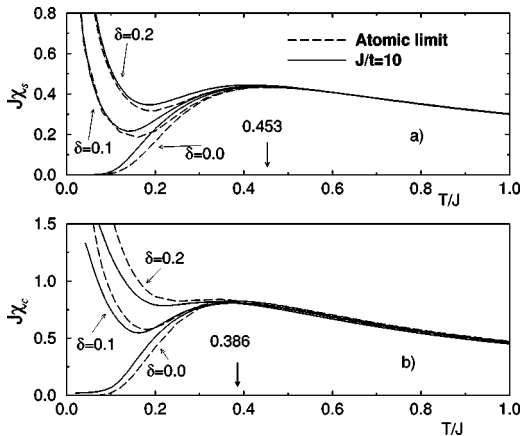

FIG. 4. Spin (a) and charge (b) susceptibilities χ_s, χ_c vs T/J calculated numerically at $J/t = 10$ (full lines). Dashed curves represent results obtained in the atomic limit. Positions of the peaks T_s in (a) and T_{qp} in (b) in the atomic limit and zero doping are indicated with arrows.
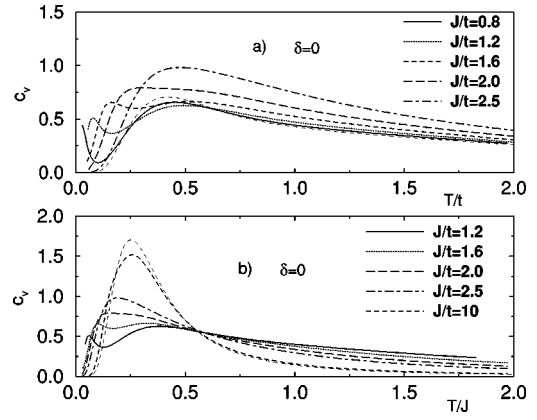

FIG. 5. Specific heat at $\delta = 0$ c_v (a) vs T/t and (b) vs T/J calculated on a system of $N_s = 10$. The faint dashed line represents the free electron result (a) and result obtained in the atomic limit (b).

singular and appears only for $T \to 0$. At small values of J, e.g., $J/t = 0.8$, 1.2, 1.6, and 2.0, we observe two peaks in c_v. The low-T peak that has emerged from the lifting of the degeneracy at $J/t = 0$ can be attributed to spin excitations. With increasing J this peak shifts towards higher T and broadens. The broadening is due to the spin excitation spectrum having bandwidth of some effective J_{eff} which increases with J. The broad peak, that originated from the free electron band at $J = 0$, shifts towards higher T with increasing J and becomes even broader. This is due to the interplay of band effects and the charge gap that develops with increasing J/t. The two peaks above $J/t = 2.5$ merge into a single peak which in the strong coupling limit scales linearly with J. At $J/t = 10$ c_v closely follows analytical prediction calculated within the atomic limit as seen in Fig. 5(b) where c_v is presented as a function of T/J. Our results for the 2D lattice are in many respects similar to results for the 1D lattice obtained by the DMRG method.[13,15]

At finite doping, $\delta = 0.1$ shown in Fig. 6(a), small peaks due to the spin gap are still visible at small T. At even larger doping, $\delta = 0.2$ shown in Fig. 6(b), new peaks emerge at very small temperatures [see also the inset of Fig. 6(b)]. These peaks shift towards larger temperatures with increasing J. The shift is approximately quadratic in J. We believe that the
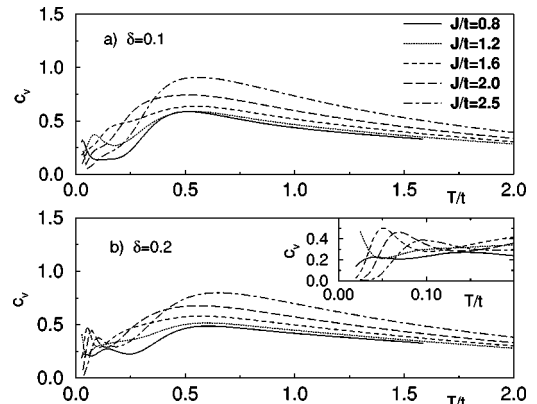

FIG. 6. Specific heat c_v T/t at (a) $\delta = 0.1$ and (b) $\delta = 0.2$ calculated on a system of $N_s = 10$. The inset represents the expanded low-temperature region in (b).

same low energy scale that gives rise to these peaks is responsible for saturation of spin susceptibility seen in the intermediate coupling J/t and $\delta = 0.2$.

IV. CONCLUSIONS

We have investigated finite-temperature properties of the Kondo lattice model on small square lattices. The chemical potential at low temperatures shows singular behavior as a function of doping. The jump in the chemical potential is a consequence of the quasiparticle gap at zero doping. The quasiparticle gap scales approximately as $\Delta_{qp} \sim 0.3J$ in the intermediate coupling regime, i.e., $1.6 \leqslant J/t \leqslant 2.5$. Similar scaling was recently found by quantum Monte Carlo simulations[19] which furthermore show that scaling persists even below the transition to the AFM state, $J/t \sim 1.4$. In the strong coupling regime the quasiparticle gap again scales linearly with J as $\Delta_{qp} \sim 0.75J$ which is not too surprising since in this case physics becomes local and J is then the only energy scale in the system. The crossover between the two linear regimes occurs when the spin gap overcomes the quasiparticle gap, i.e., at $J/t > 2.5$. Interestingly, calculations in 1D show two distinct linear regimes for the charge gap vs J/t.[10]

Two temperature scales govern the temperature dependence of spin susceptibility in the intermediate coupling regime. One scale is given by $T_c/J \sim 0.6$ above which we find an almost perfect scaling calculated for a wide range of J. One possible explanation of this unusual scaling is that T_c is governed by the charge gap Δ_c. We have shown in the previous section that the quasiparticle gap at the intermediate

coupling scales as $\Delta_{qp} \sim 0.3J$. Assuming $\Delta_c = 2\Delta_{qp}$ we get a linear scaling for the charge gap, $\Delta_c \sim 0.6J$, which agrees with the value for T_c. At lower temperatures $T \sim T_s$, physics at zero doping is governed by the spin gap Δ_s. This remains true as long as $\Delta_s < \Delta_{qp}$. Near the strong coupling regime the opposite becomes true, then the quasiparticle gap determines the low-temperature physics of the spin susceptibility.

The charge susceptibility shows substantially different behavior than the spin susceptibility. On a smaller system of $N_s = 8$ we find scaling with J in the whole temperature range within the intermediate Kondo coupling region. This result suggests that a single energy scale, identified as a quasiparticle gap $\Delta_{qp} \sim 0.3J$, governs the physics of the charge response of the system.

At finite doping we find a new energy scale. It is reflected in the saturation of the $1/T$ behavior in $\chi_s(T)$ at small temperatures and in the appearance of low-temperature peaks in the specific heat c_v at $\delta = 0.2$. Approximate quadratic scaling of the position of the peaks in c_v with the Kondo coupling strength suggests, that this energy scale could be attributed to the RKKY interaction between uncompensated spins at finite doping.

[1] H. Tsunetsugu, M. Sigrist, and K. Ueda, Rev. Mod. Phys. **69**, 809 (1997).

[2] M. Sigrist, H. Tsunetsugu, K. Ueda, and T.M. Rice, Phys. Rev. B **46**, 13 838 (1992).

[3] N. Read, D.M. Newns, and S. Doniach, Phys. Rev. B **30**, 3841 (1984).

[4] P. Coleman, Phys. Rev. B **29**, 3035 (1984).

[5] P. Fazekas and E. Müller-Hartmann, Z. Phys. B **85**, 285 (1991).

[6] R. Eder, O. Stoica, and G.A. Sawatzky, Phys. Rev. B **55**, R6109 (1997); **58**, 7599 (1998).

[7] H. Tsunetsugu, Y. Hatsugai, K. Ueda, and M. Sigrist, Phys. Rev. B **46**, 3175 (1992).

[8] S.R. White, Phys. Rev. Lett. **69**, 2863 (1992).

[9] C.C. Yu and S.R. White, Phys. Rev. Lett. **71**, 3866 (1993).

[10] N. Shibata, T. Nishino, K. Ueda, and C. Ishii, Phys. Rev. B **53**, R8828 (1996).

[11] N. Shibata, J. Phys. Soc. Jpn. **66**, 2221 (1997).

[12] X. Wang and T. Xiang, Phys. Rev. B **56**, 5061 (1997).

[13] N. Shibata, B. Ammon, M. Troyer, M. Sigrist, and K. Ueda, J. Phys. Soc. Jpn. **67**, 1086 (1998).

[14] N. Shibata and H. Tsunetsugu, J. Phys. Soc. Jpn. **68**, 744 (1999).

[15] N. Shibata and K. Ueda, J. Phys.: Condens. Matter **11**, R1 (1999).

[16] T. Mutou, N. Shibata, and K. Ueda, Phys. Rev. Lett. **81**, 4939 (1999).

[17] Z. Wang, X.P. Li, and D.H. Lee, Physica B **199-200**, 463 (1994).

[18] Z.P. Shi, R.R.P. Singh, M.P. Gelfand, and Z. Wang, Phys. Rev. B **51**, 15 630 (1995).

[19] F.F. Assaad, Phys. Rev. Lett. **83**, 796 (1999).

[20] *Phase Transitions and Critical Phenomena*, edited by C. Domb and M.S. Green (Academic, London, 1974).

[21] J. Jaklič and P. Prelovšek, Phys. Rev. Lett. **77**, 892 (1996); J. Jaklič and P. Prelovšek, Adv. Phys. **49**, 1 (2000).